Supplemental Material for Chapter 2

Contents of this file

Introduction

Supplementary texts S1-S8 detail relevant changes to microphysics or model setup between DYAMOND 1 and 2, expanding on the information provided in Table 2 in the main text. Supplementary figures S1-S3 provide extra information to plots in the main text for the curious reader.

Text S1. ARP

The configuration of ARP was similar to the DYAMOND 1 simulation save for “an important improvement using microphysics from the LAM model AROME, specially tuned for high resolution non-hydrostatic modeling." (DYAMOND website; https://easy.gems.dkrz.de/DYAMOND/Winter/Models/description/ARPEGE.html)

Text S2. GEOS

In DYAMOND 1, the microphysics used in GEOS was not representative of the current state of the model (personal communication with **William** Putman). Thus, we removed GEOS DYAMOND 1 from our analysis.

Text S3. FV3/SHiELD

Between DYAMOND 1 and DYAMOND 2, FV3 had significant model development to become the eXperimental DYAMOND-class global storm resolving model (X-SHiELD), which is part of the unified forecast system from NOAA’s Geophysical Fluid Dynamics Lab (GFDL). A noteable change in the microphysics is related to the terminal velocity of ice, which can impact tropical cirrus by influencing the amount of cloud ice (personal communication with Linjiong Zhou and Lucas Harris, GFDL).

Text S4. ICON

No significant changes.

Text S5. IFS

The IFS model versions used for DYAMOND 1 and 2 are CY45R1 and CY47R1 respectively. The differences between the two runs can be found in their documentation.

Excerpts here from “Physical Processes” (ECMWF 2018; ECMWF 2020a)

- Chapter 2. Corrected and expanded descriptions of the cloud droplet and ice particle effective radii in the radiation scheme.
- Chapter 6. Added moisture convergence closure, expanded coupling to the cloud scheme. Added descriptions and derivations for new Grib fields (new CAPE/CIN, tropopause height)
- Chapter 7. Added new microphysics processes. Revised precipitation type. Revised cloud scheme section, precipitation type description.

Excerpts from “Dynamical and Numerical Procedures” (ECMWF 2020b)

- New sponge at the model top

Text S6. NICAM

The DYAMOND 2 simulation with NICAM included an inaccurate representation of snow over land and a poorly-performing microphysics scheme over land. The NICAM model

output was removed from the host server and we removed it from our analysis for DYAMOND 2.

Text S7. SAM

SAM in DYAMOND 1 had a “wall” at 89°N/S. This was fixed for the DYAMOND 2 run by having a singularity at the pole using triangular grids (but larger grid boxes); the horizontal grid spacing is minimized in the mid-latitudes (with 4.25km resolution at the equator). Furthermore, the temperature profile used for precipitation-related coefficients changed from one standard profile in DYAMOND 1 to a local 3D profile in DYAMOND 2 (Khairoutdinov, 2022).

Text S8. UM

No significant changes.

Table S1. Mean OLR (in W/m2) for global tropics (GT; 30°N-30°S) and the TWP (143°E-153°E; 5°N-5°S) regions. The relative local difference for the TWP is shown in the third column as the difference between the GT and TWP regions relative to the difference observed using CERES data. The models are ordered from a cool bias (low OLR) in the TWP to a warm bias (high OLR).

Model	GT	TWP	Relative local difference
MPAS	251	175	-42
UM	265	199	-15
CERES	**257**	**213**	**0**
SHiELD	262	219	+5
GEOS	269	223	+9
SAM	272	232	+19
ICON	266	237	+24
SCREAM	268	245	+32
ARP	253	248	+35
IFS	269	265	+52

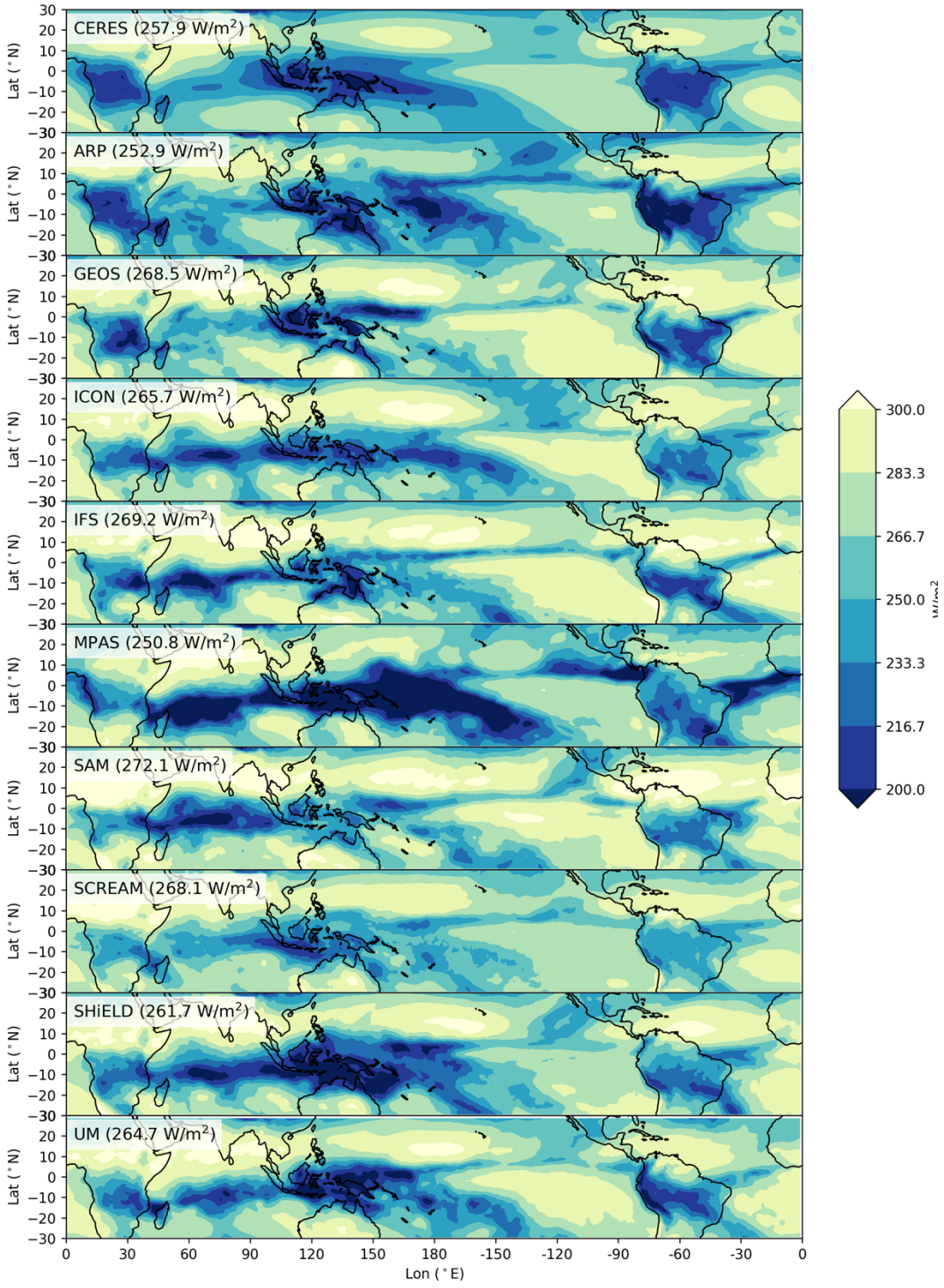

Figure S1. The top panel shows mean OLR for observations from CERES SYN1deg data from January, February, and March of 2001-2013. The panels below show the mean OLR from the models' last 30 days of the simulation. The model and spatiotemporal mean of OLR is noted in the upper left of each panel.

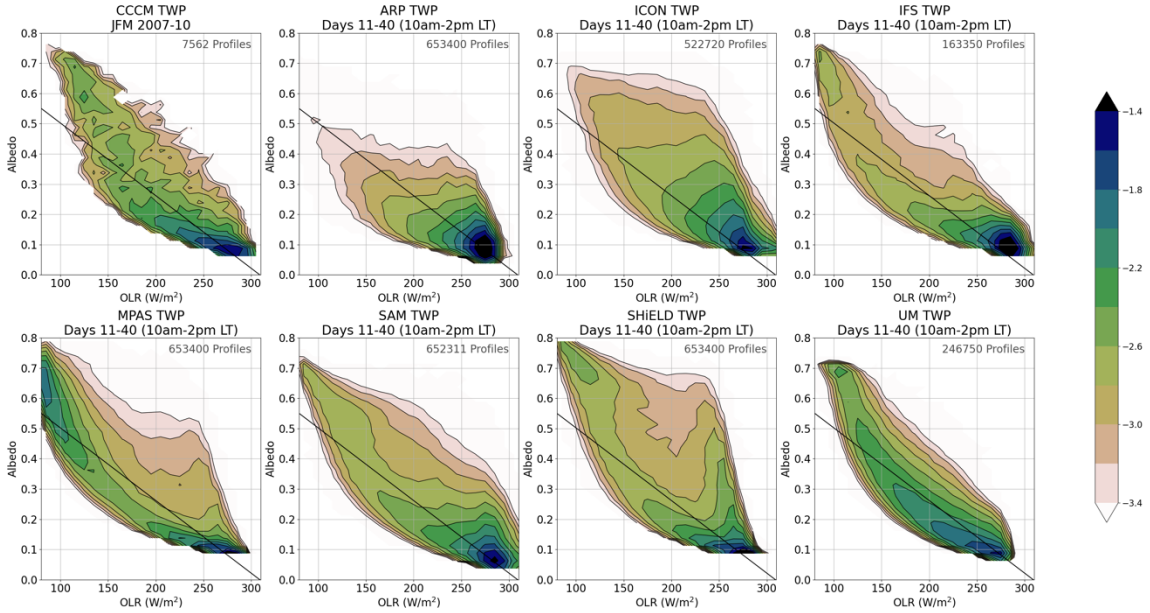

Figure S2. Joint albedo-OLR histogram is shown for observations from January, February, and March of 2008-2011 in the top left panel. The other panels show the joint albedo-OLR histogram for the models from DYAMOND 2 (days 10-40). The colorbar shows the log of the probability distribution.

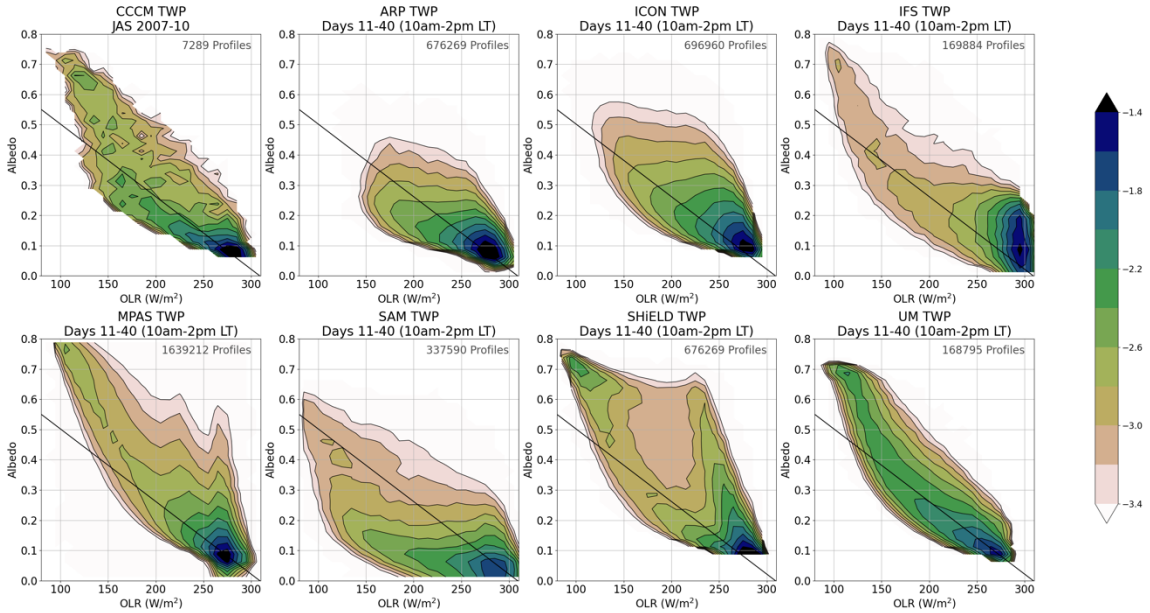

Figure S3. Joint albedo-OLR histogram is shown for observations from July, August, and September of 2007-2010 in the top left panel. The other panels show the joint albedo-OLR histogram for the models from DYAMOND 2 (days 10-40). The colorbar shows the log of the probability distribution.

References

ECMWF. (2018). IFS Documentation CY45R1 - Part IV: Physical processes [Technical]. DOI: 10.21957/4whwo8jw0

ECMWF. (2020a). IFS Documentation CY47R1 - Part IV: Physical Processes [Technical]. DOI: 10.21957/cpmkqvhja

ECMWF. (2020b). IFS Documentation CY47R1 - Part III: Dynamics and Numerical Procedures [Technical]. DOI: 10.21957/u8ssd58

Khairoutdinov, M. F., Blossey, P. N., & Bretherton, C. S. (2022). Global System for Atmospheric Modeling: Model Description and Preliminary Results. *Journal of Advances in Modeling Earth Systems,* 14(6), e2021MS002968. DOI: 10.1029/2021MS002968